Journal of Solid State Chemistry 181 (2008) 2378–2385

Contents lists available at ScienceDirect

Journal of Solid State Chemistry

journal homepage: www.elsevier.com/locate/jssc

Hydrothermal syntheses, crystal structures and properties of three coordination frameworks based on a new semirigid ligand and benzenedicarboxylate

Yao-Mei Fu, Ya-Hui Zhao, Ya-Qian Lan, Kui-Zhan Shao, Yong-Qing Qiu *, Xiang-Rong Hao, Zhong-Min Su *

Faculty of Chemistry, Institute of Functional Material Chemistry, Northeast Normal University, No. 5268 Renmin Street, Changchun 130024, China

ARTICLE INFO

Article history:
Received 8 December 2007
Received in revised form
8 May 2008
Accepted 24 May 2008
Available online 1 June 2008

Keywords:
Semirigid ligand
2,2′-Biimidazole
Hydrothermal reaction
Crystal structure
Fluorescent property

ABSTRACT

Three novel polymers, $\{[Cd(m\text{-bdc})(\mathbf{L})]\cdot H_2O\}_n$ (**1**), $[Co(m\text{-bdc})(\mathbf{L})_{0.5}(H_2O)]_n$ (**2**) and $[Zn_5(\mathbf{L})_2(p\text{-bdc})_5(H_2O)]_n$ (**3**) based on 1,1′-bis(pyridin-3-ylmethyl)-2,2′-biimidazole (**L**) ligand and benzenedicarboxylate isomers, have been prepared and structurally characterized. Compound **1** exhibits a 2D architecture with $(4^2\cdot6)(4^2\cdot6^7\cdot8)$ topology, which is synthesized by **L** and 1,3-benzenedicarboxylate (*m*-bdc) ligands. Compound **2** is constructed from 1D chains that are linked by **L** ligands extending a 2D (4,4) grid. Compound **3** is a 3D framework with $(4^3)(4^6\cdot6^{18}\cdot8^4)$ topology, which is composed of trinuclear clusters and five-coordinated metal centers joined through 1,4-benzenedicarboxylate (*p*-bdc) and **L** ligands. Moreover, the fluorescent properties of **L** ligand, compounds **1** and **3** are also determined.

1. Introduction

Metal organic frameworks (MOFs) have received much attention in the field of supramolecular chemistry and crystal engineering because of their diverse structures and promising applications in catalysis, nonlinear optics, luminescent materials, porous materials and microelectronics [1–5]. It is well-known that the structural and functional information of such target materials significantly relies on the metal and ligand precursors. In this case, the design of new types of ligands for constructing unusual MOFs is obviously not trivial at this stage and a variety of organic ligands containing nitrogen donor or oxygen donor have been intensely investigated due to their excellent coordination abilities [6,7]. Nowadays, increasing attention has been focused on flexible or semirigid ligands because they can change their conformations according to the requirements of different metal atoms and may induce structures with novel topologies or properties [8]. Some novel structures such as helical, interpenetrating frameworks constructed from flexible ligands have been obtained [9–12]. Meanwhile, the use of ligand with multiple flexible arms containing coordination sites has also aroused people's interests recently [13], and variation in the category and relative arrangement of the arms in this ligand might be expected to generate assemblies of varying dimensionalities with novel structural and functional properties.

2,2′-Biimidazole (H_2biim) has received much attention because of its potential applications in supramolecular chemistry, biochemistry, cluster science and antitumor drugs [14]. However, designing and constructing novel MOFs from the derivatives of H_2biim remain largely unexplored [15–17]. With the aim of preparing new materials with beautiful architectures and as a continuing study of H_2biim [18], we have synthesized a new two-armed ligand based on H_2biim, that is 1,1′-bis(pyridin-3-ylmethyl)-2,2′-biimidazole (**L**) (Scheme 1). **L** ligand possesses interesting features that are helpful to the formation of versatile coordination structures: (I) **L** is a modified version of H_2biim and more flexible than H_2biim because of the presence of the $-CH_2-$ spacer between H_2biim and pyridyl units and can change its conformational geometry according to the demands of metal centers. (II) **L** ligand can provide two kinds of nitrogen atoms to coordinate with metal atoms, namely, nitrogen atom from the imidazole ring (N_{im}) and nitrogen atom from the pyridyl ring (N_{py}). Recently, Kim, Hupp and Chen reported a series of porous MOFs constructed from mixed organic linkers, exhibiting interesting properties [19–21]. Enlightened by them and to facilitate the generation and crystallization of metal complexes with the **L**

---

* Corresponding authors. Fax: +86 431 85099291.
E-mail address: Qiuyq466@nenu.edu.cn (Y.-Q. Qiu).

0022-4596/$ - see front matter © 2008 Elsevier Inc. All rights reserved.
doi:10.1016/j.jssc.2008.05.039

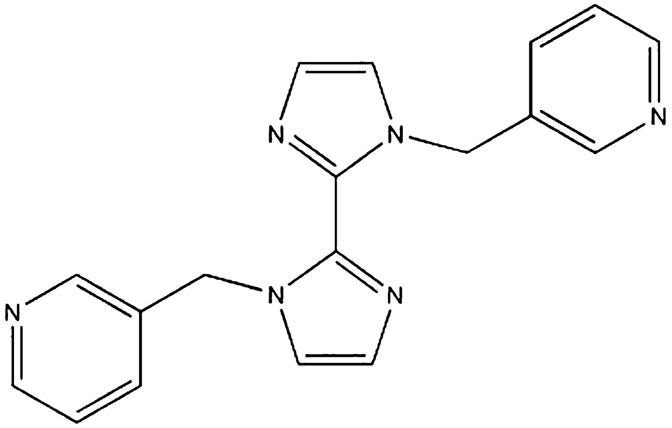

Scheme 1. 1,1′-Bis(pyridin-3-ylmethyl)-2,2′-biimidazole (**L**).

ligand, we introduce benzenedicarboxylate (bdc) isomers (*m*-bdc and *p*-bdc) as co-ligands to prepare new inorganic–organic hybrid materials. First, bdc isomers exhibit versatile coordination behavior and some examples constructed from bdc isomers have been reported [22,23]. Second, bdc isomers contain two carboxyl groups at distinct positions, which may engender significant special effect and may induce novel structures. Finally, the deprotonated carboxyl groups can act as anionic organic ligands to coordinate with the metal center as well as to compensate the charge [24]. The possibility of **L** and bdc ligands to coordinate with metal ions potentially allows access to frameworks of novel topologies. Additionally, MOFs constructed from mixed ligands might be expected to exhibit useful properties or beautiful topologies.

In this paper, three unprecedented MOFs have been obtained and characterized by single-crystal X-ray diffraction, which are assembled by transition metal ions combined with **L** ligand and bdc isomers in different molar ratios. Compared with complexes constructed from H_2biim and bdc ligands, there are many differences in the three compounds, which may be due to the steric effect and different coordination modes of **L** and bdc ligands. Herein, we report the syntheses and single-crystal X-ray structural characterizations of the three compounds. The XRPD for compounds **1** and **3** and the infrared spectra for compounds **1**–**3** have also been examined. Compound **1** is a 2D binodal (3,5)-connected structure with $(4^2 \cdot 6)(4^2 \cdot 6^7 \cdot 8)$ topology, which is constructed from cadmium salt, **L** and *m*-bdc ligands. Compound **2** is constructed from 1D chains formed by dinuclear subunits and the 1D chains are linked by the **L** ligand exhibiting a 2D (4,4) grid. Compound **3** is a 3D binodal (3,8)-connected network and its Schläfli symbol is $(4^3 \cdot 6^3)(4^6 \cdot 6^{18} \cdot 8^4)$ topology. Moreover, fluorescent properties of the **L** ligand, compounds **1** and **3** are also examined in the solid state, indicating that they may be suitable as candidates of fluorescent materials.

2. Experimental section

The reagents and solvents were commercially available and used as received without further purification. H_2biim was prepared according to the reported procedure [25]. Elemental analyses (C, N and H) were performed on a Perkin-Elemer 2400 CHN elemental analyzer. FT-IR spectra were recorded in the range 400–4000 cm^{-1} on an Alpha Centaurt FT/IR Spectrophotometer as KBr pellets. All measurements were performed at room temperature. The X-ray powder diffraction (XRPD) patterns were recorded on a Siemens D5005 diffractometer with Cu KR ($\lambda = 1.5418$ Å) radiation. The emission/excitation spectra were recorded on a Varian Cary Eclipse spectrometer.

2.1. Synthesis of the **L** ligand

The **L** ligand was synthesized according to the reported literature [26]. To a solution of H_2biim (1 mmol) in 15 mL DMSO was added 2 mmol 3-picolyl chloride hydrochloride and 4 mmol NaOH. After the reaction mixture was stirred for 10 h at 50–60 °C, the solvent was removed under vacuum. The rest were dissolved in 50 mL water and then extracted by dichloromethane. The organic layer was dried by anhydrous $MgSO_4$ and then filtered. After evaporating the solvent of dichloromethane, the products would be obtained yielded by 70%.

2.2. Syntheses of complexes

$\{[Cd(m\text{-bdc})(\mathbf{L})] \cdot H_2O\}_n$ (**1**): A mixture of $Cd(OAc)_2 \cdot 2H_2O$ (0.2 mmol), **L** (0.2 mmol), *m*-bdc (0.2 mmol), NaOH (0.4 mmol), and H_2O (9 mL) was placed in a 14 ml Teflon-lined stainless steel vessel, and then the vessel was sealed and heated at 150 °C for 3 days. After the reaction mixture was slowly cooled down to room temperature at the rate of 5 °C/h, colorless block crystals of compound **1** were obtained. Yield: 70%. Anal. Calcd. for $C_{104}H_{80}N_{24}O_{20}Cd_4$: C, 51.29; H, 3.31; N, 13.80. Found C, 51.13; H, 3.35; N, 13.86. IR (cm^{-1}): 3422 (w), 3106 (w), 1194 (w), 1131 (w), 61 (w), 1480 (m), 1432 (m), 1278 (m), 717 (m), 1603 (s), 1551 (s), 1386 (s), 750 (s).

$[Co(m\text{-bdc})(\mathbf{L})_{0.5}(H_2O)]_n$ (**2**): A mixture of $Co(OAc)_2 \cdot 2H_2O$ (0.2 mmol), **L** (0.1 mmol), *m*-bdc (0.2 mmol), NaOH (0.4 mmol), and H_2O (9 mL) was placed in a 14 mL Teflon-lined stainless steel vessel, and then the vessel was sealed and heated at 150 °C for 3 days. After the reaction mixture was slowly cooled down to room temperature at the rate of 5 °C/h, purple block crystals of compound **2** were obtained. Yield: 50%. Anal. Calcd. for $C_{34}H_{28}N_6O_{10}Co_2$: C, 51.14; H, 3.53; N, 10.52. Found C, 51.04; H, 3.37, N, 10.46. IR (cm^{-1}): 3439 (w), 1574 (w), 1483 (w), 1274 (w), 1538 (m), 1443 (m), 1608 (s), 1396 (s), 735 (s).

$[Zn_5(\mathbf{L})_2(p\text{-bdc})_5(H_2O)]_n$ (**3**): A mixture of $Zn(OAc)_2 \cdot 2H_2O$ (0.5 mmol), **L** (0.2 mmol), *p*-bdc (0.5 mmol), NaOH (1.0 mmol), and H_2O (9 mL) was placed in a 14 mL Teflon-lined stainless steel vessel, and then the vessel was sealed and heated at 150 °C for 3 days. After the reaction mixture was slowly cooled down to room temperature at the rate of 5 °C/h, colorless block crystals of compound **3** were obtained. Yield: 65%. Anal. Calcd. for $C_{76}H_{56}N_{12}O_{22}Zn_5$: C, 50.26; H, 3.11; N, 9.25. Found C, 50.02; H,

Table 1
Crystal data and structure refinement for compounds **1**–**3**

Complex	**1**	**2**	**3**
Empirical formula	$C_{26}H_{20}N_6O_5Cd$	$C_{17}H_{14}N_3O_5Co$	
$C_{76}H_{56}N_{12}O_{22}Zn_5$ 1816.28	Formula weight	608.88	399.24
Crystal system	Monoclinic	Triclinic	Triclinic
Space group	*P*21/*c*	*P*−1	*P*−1
a (Å)	14.0452(10)	8.830(5)	9.953(3)
b (Å)	8.9061(7)	10.010(5)	13.276(4)
c (Å)	20.0847(15)	10.839(5)	16.945(5)
β (deg)	97.3740(10)	67.916(5)	76.527(5)
V (Å3)	2491.6(3)	772.2(7)	1954.3(9)
Z	4	2	1
μ (mm^{-1})	0.93	1.15	1.594
T (K)	293(2)	293(2)	293(2)
Final R_1, wR_2 $[I > 2\sigma(I)]$[a]	0.0419, 0.1103	0.0290, 0.0697	0.0322, 0.0726
Final R_1, wR_2 (all data)[b]	0.0715, 0.1272	0.0333, 0.0725 0.0448,	0.0785

[a] $R_1 = \Sigma \| F_0 | - | F_c \| / \Sigma || F_0 |$.

[b] $wR_2 = \Sigma[w(F_0^2 - F_c^2)2] / \Sigma[w(F_0^2)^2]^{1/2}$.

3.21; N, 9.31. IR (cm^{-1}): 3423 (w), 3130 (w), 828 (w), 575 (w), 546 (w), 1508)m), 1290 (m), 675 (m), 1640 (s), 1610 (s), 1584 (s), 1396 (s), 749 (s).

2.3. Crystal structure determinations

X-ray single-crystal diffraction data for complexes **1**–**3** were performed with grasphite-monochromated Moka radiation. Reflection was collected with a Bruker Smart Apex detector. The structures were solved by direct methods and refined on F^2 using **SHELXTL-97** [27]. All non-hydrogen atoms were refined anisostropically by full-matrix least-squares methods. The hydrogen atoms were added geometrically and not refined. Further details of X-ray structure analyses are given in Table 1, and selected bond distances and angles for **1**, **2** and **3** are listed in Table S1–Table S3.

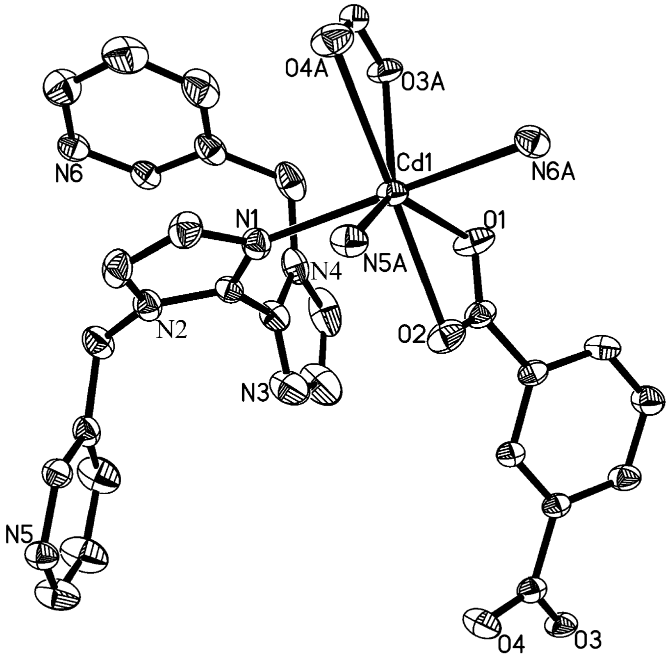

Fig. 1. ORTEP drawing of the coordination environment of cadmium ion in compound **1** with thermal ellipsoids at the 30% probability level. H atoms and sovent water molecule are not shown for clarity.

3. Results and discussion

3.1. Crystal structures of compounds 1–3

When the **L** ligand, the *m*-bdc ligand and $Cd(OAc)_2 \cdot 2H_2O$ were used as materials, compound **1** was obtained. Single-crystal X-ray diffraction analysis reveals that compound **1** is a 2D framework. As shown in Fig. 1, the structure contains one crystallographically unique cadmium center bonded by seven atoms furnishing a distorted pentagonal bipyramidal geometry completed by three nitrogen atoms from three **L** ligands and four oxygen atoms of two carboxylate groups from two *m*-bdc ligands (Cd1–N1 = 2.364(3) Å, Cd1–N6A = 2.428(3) Å, Cd1–O1 = 2.390(3) Å, Cd1–O2 = 2.413(3) Å, Cd1–O3B = 2.296(2) Å, Cd1–O4B = 2.614(3) Å, Cd1–N5C = 2.407(3) Å). The distances accord with the reported compounds [28].

Each **L** acting as a tri-connector coordinates with three metal centers through two N_{py} and one N_{im} donors forming a 1D irregular ladder-like chain. Two imidazole rings of the **L** ligand are not in the same plane, which have the dihedral angle of 70.95° compared with the reported complexes constructed from the H_2biim ligand [29,30]. Because of the existence of the $-CH_2-$ spacer between the pyridyl ring and the H_2biim unit, the **L** ligand exhibits its flexibility and two pyridyl rings are almost vertical to each other, having the dihedral angle of 82.79°. Each *m*-bdc ligand in structure **1** bonds with two metal atoms in the bis-chelating coordination mode (Scheme 2a) forming a wave-like 1D chain viewed along the *a*-axis and the chains are further interweaved by 1D ladder-like chains built from the **L** ligand, resulting in a 2D network (Fig. 2).

A better insight into the nature of the framework can be achieved by the application of a topological approach. Each metal center in compound **1** is bonded with three **L** ligands and two caboxylate groups from two *m*-bdc ligands forming a 5-connected node. Each **L** ligand connects three metal centers acting as a

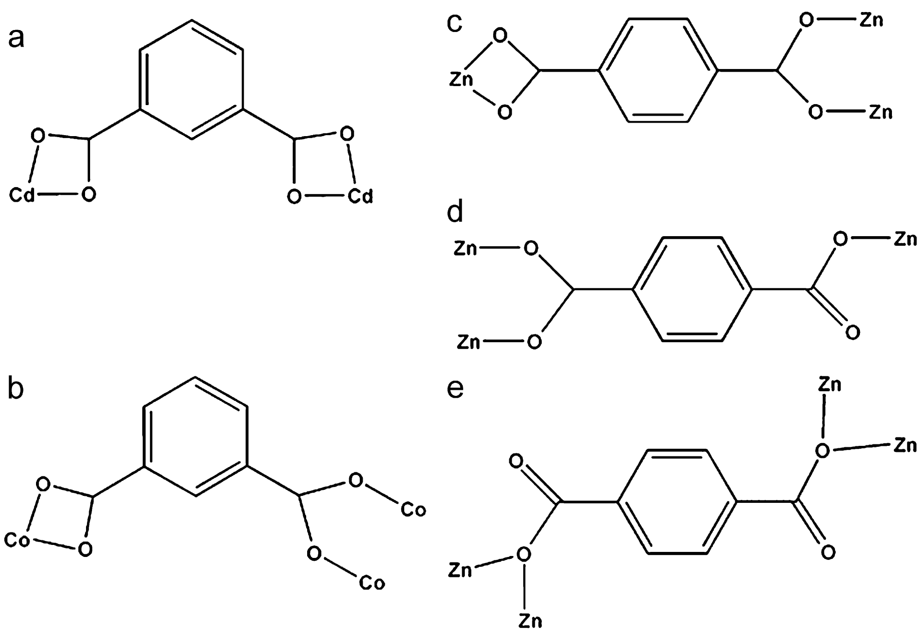

Scheme 2. Coordination modes of *m*-bdc and *p*-bdc ligands in compounds **1**–**3**.

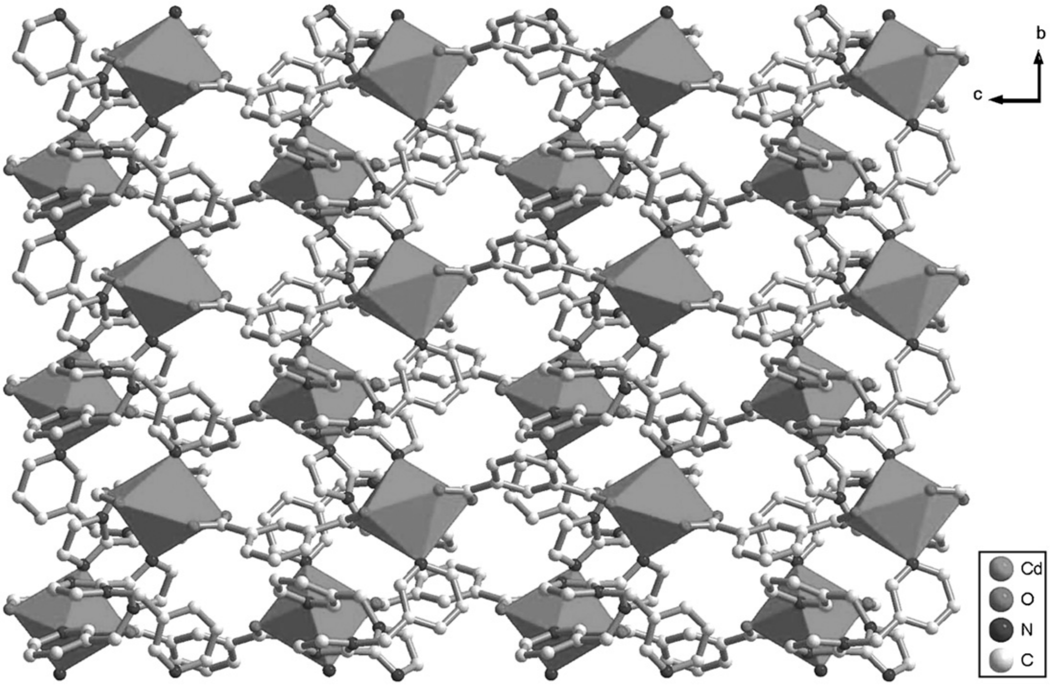

Fig. 2. View of the 2D structure of compound **1** in a polyhedral representation.

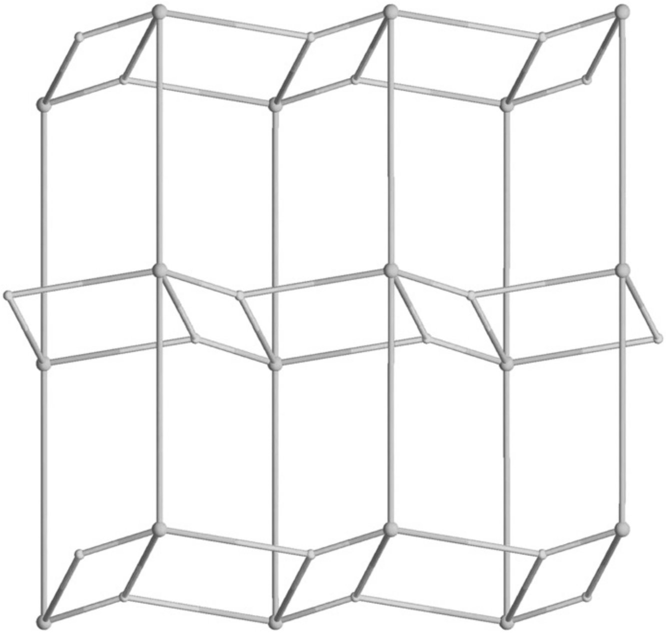

Fig. 3. Topological view of the 2D framework of compound **1**.

3-connected node. So the whole framework can be described as a (3,5)-connected net with the Schläfli symbol of $(4^2 \cdot 6)(4^2 \cdot 6^7 \cdot 8)$ (the first is for the 3-connected **L** ligand and the second symbol for the 5-connected cadmium center) shown in Fig. 3. Although a large number of examples of three-, four- or six-connected networks have been reported, to our knowledge, networks of five connected are rare and especially few examples of binodal topology containing five connected have been explored [31–34]. This example indicates that topological analysis is a useful tool for the description of network.

To investigate the coordination chemistry of **L** and *m*-bdc ligands with $Co(OAc)_2 \cdot 2H_2O$, compound **2** was synthesized, which exhibits a 2D (4,4) sheet. The coordination environment of the asymmetric unit is shown in Fig. 4. The Co(II) is six-coordinated by five oxygen atoms and one nitrogen atom furnishing a distorted octahedral geometry. The equatorial plane is occupied by O1, O2, O3A and O4A from three different carboxylate groups of three different *m*-bdc ligands (Co1–O1 = 1.9981(16) Å, Co1–O2 = 2.0389(16) Å, Co1–O3A = 2.1084(15) Å, Co1–O4A = 2.2517(18) Å), and the apical sites are completed by N_{py} of **L** ligand and O1W from the water molecule (Co1–N1 = 2.1673(18) Å, Co1–O1W = 2.1618(17) Å). The bond distances are comparable to the reported results [35].

Similar to the 4,4′-bipyridine ligand, the **L** ligand also acts as a bidentate ligand through its two N_{py} donors linking two metal ions, while two N_{im} donors do not participate in coordinating with metal ions. Two imidazole rings of the **L** ligand in structure **2** are in the same plane and two pyridyl rings in one **L** ligand are parallel to each other, while in compound **1** it has large dihedral angles. Different from compound **1**, each *m*-bdc ligand in compound **2** connects with three cobalt centers in the chelating–bridging coordination mode (Scheme 2b) forming a $[Co(m\text{-bdc})]_n$ chain formed by $\{Co_2\}$ subunits (Fig. 5a), and the 1D chain is banded by different **L** ligands that are orientated in opposite directions extending a 2D layer depicted in Fig. 5b. The $\{Co_2\}$ binuclear structural units with the distance of Co–Co = 4.395 Å are formed by bridging carboxylate groups from two different *m*-bdc ligands, which in turn are linked to each other through the chelating carboxylate groups of *m*-bdc ligands similar to that of $\{[Co(ip)(bpmp)] \cdot H_2O\}$ [36], where 1D chains are linked into a 2D framework through the **L** ligand. If the binuclear units are regarded as a node, the whole framework of compound **2** can be viewed as the common (4,4) grid (Fig. 6). Different from compound **1**, the chelating–bridging coordination mode of *m*-bdc in compound **2** induces the formation of binuclear subunits and the bi-connector of **L** ligand contributes to the construction of the 2D framework.

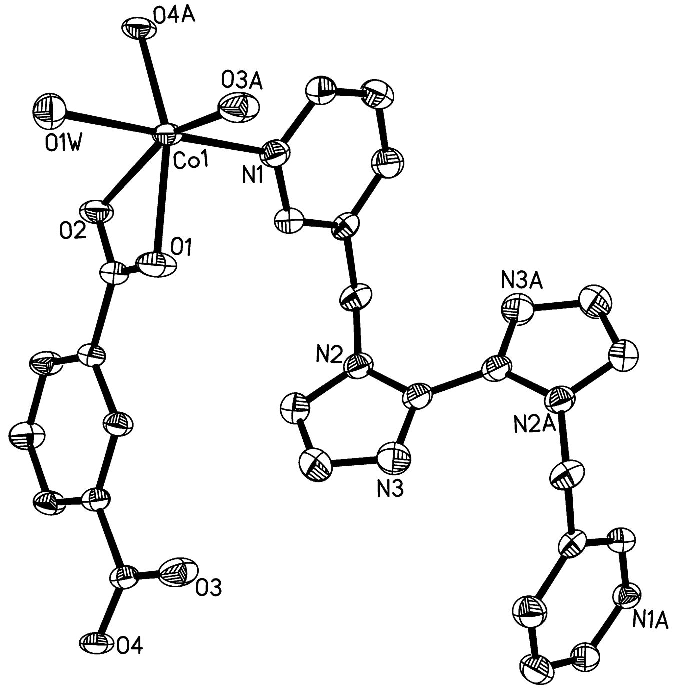

Fig. 4. ORTEP drawing of the coordination environment of cobalt ion in compound **2** with thermal ellipsoids at the 50% probability level. H atoms are not shown for clarity.

Single-crystal X-ray diffraction analysis reveals that compound **3** is a 3D framework constructed from **L** and *p*-bdc ligands. There exist three crystallographic independent zinc centers and their coordination environments are shown in Fig. 7. The Zn1 ion is coordinated with six oxygen atoms derived from six carboxylate groups, which is located in an inversion center. The coordination environment of Zn1 is a regular octahedral coordination sphere completed by six oxygen atoms from six *p*-bdc ligands (Zn1–O1 = Zn1–O1A = 2.1980(14) Å, Zn1–O5 = Zn1–O5A = 2.0677(15) Å, Zn1–O4 = Zn1–O4A = 2.0729(15) Å). While Zn2 is in a tetrahedral coordination sphere completed by three oxygen atoms O1, O3, O6 from three *p*-bdc ligands and one N_{im} atom (Zn2–O1 = 1.9684(14) Å, Zn2–O3 = 1.9534(15) Å, Zn2–O6 = 1.9826(16) Å, Zn2–N2 = 1.9928(18) Å). Different from Zn1 and Zn2, Zn3 is bonded by four oxygen atoms and one nitrogen atom forming a distorted trigonal–bipyramidal coordination geometry completed by four oxygen atoms derived from two *p*-bdc ligands and two water molecules, and one N_{py} from the **L** ligand (Zn3–O10 = 2.3506(18) Å, Zn3–O9 = 2.0453(18) Å, Zn3–O8 = 1.9618(17) Å, Zn3–N1 = 2.095(2) Å, Zn3–O1W = 2.027(2) Å). The distances except for that of Zn3 and O7 are in the average ranges compared with the reported complexes [37,38], while the distance of Zn3 and O7 is 2.668 Å slightly larger than the actual bond, indicating that there exists a weaker interaction between them. Obviously, the average bond lengths around Zn2 are somewhat shorter than those of Zn1 and Zn3, which is consistent with the fact that bond lengths in a tetrahedral geometry are generally shorter than those in other geometries, which is comparable to that previously reported in the literature [39].

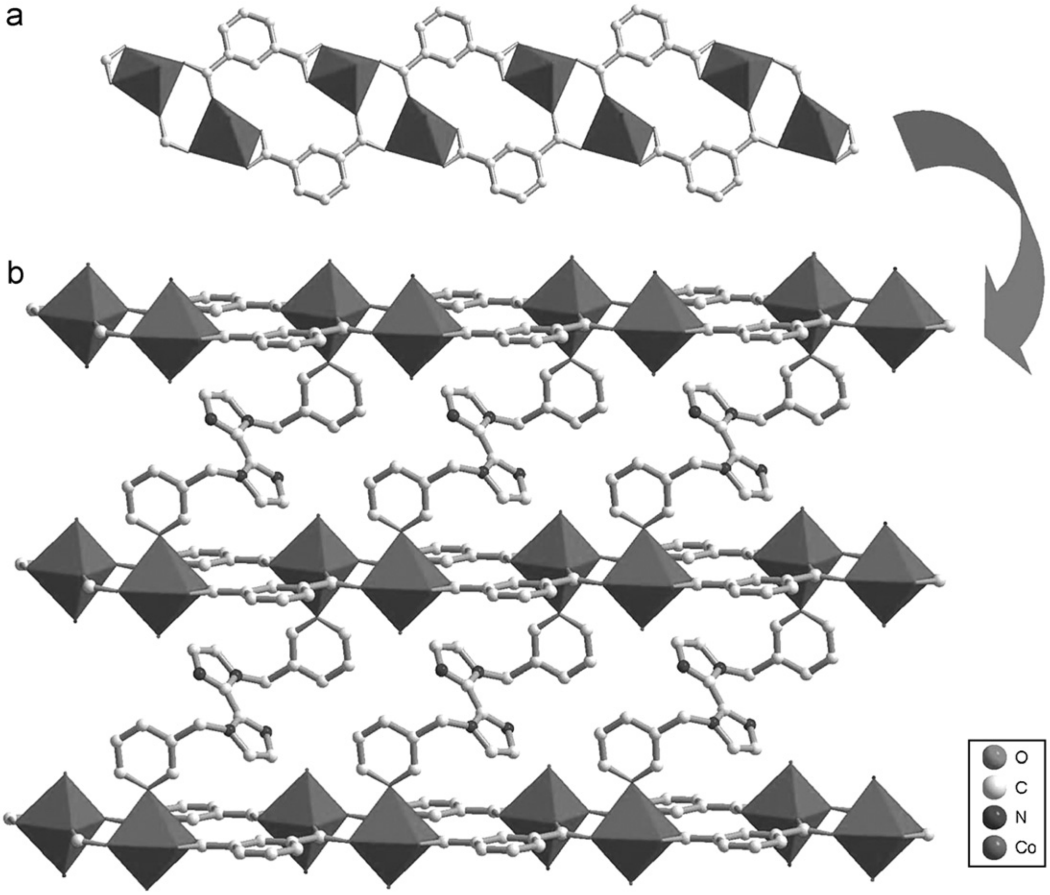

Fig. 5. (a) View of the 1D chain formed by binuclear structure units in compound **2**. (b) View of the 2D sheet of compound **2** in a polyhedral representation.

Due to the steric hindrance of **L** and the coordination demand of zinc ion, the **L** ligand provides two nitrogen atoms (N_{im} and N_{py}) to participate in the formation of compound **3** different from compound **2,** which provides two N_{py} donors to coordinate with the metal center. Two imidazole rings of **L** have a dihedral angle of 52.13° and two pyridyl rings have a dihedral angle of 12.94° smaller than those of compound **1**. The ligand of *p*-bdc exhibits three coordination modes (shown in Scheme 2(c)–(e)), resulting in the formation of polymer **3**. Six *p*-bdc ligands connect three zinc centers forming a linear trinuclear cluster and a similar cluster has been found in $[Cd_3(H_2biim)_2(1{,}4\text{-}bdc)_3]\cdot2H_2O$ [40], $[Co_3(bpdc)_3(bpy)]\cdot4DMF\cdot H_2O$ [41] and $[Zn_3(BDC)_3(DEF)_2]$ [42]. Each of the trinuclear clusters in compound **3** consists of a single octahedrally coordinated zinc center surrounded by two peripheral tetrahedrally coordinated zinc centers. The peripheral zinc center is bound with the central zinc atom through three bridging carboxylate groups.

It should be noted that the whole structure of compound **3** is composed of trinuclear clusters and five-coordinated metal centers joined through *p*-bdc and **L** ligands. Each of the trinuclear clusters is linked to another two trinuclear clusters through two *p*-bdc ligands and six tetrahedrally coordinated zinc centers through four *p*-bdc ligands and two **L** ligands, which defines an 8-connected node (Fig. 8a), while in the reported compound of $[Cd_3(H_2biim)_2(1{,}4\text{-}bdc)_3]\cdot2H_2O$, the similar trinuclear cluster acts as a 6-connected node. This may be due to different coordination modes of **L** and H_2biim ligands. Each five-coordinated zinc center links to three trinuclear clusters through two *p*-bdc ligands and one **L** ligand acting as a 3-connected node (Fig. 8b). Thus, compound **3** exhibits a (3,8)-connected net with the Schläfli symbol of $(4^3)(4^6\cdot6^{18}\cdot8^4)$ (the first symbol is for the 3-connected zinc center and the second for the 8-connected trinuclear) shown in Fig. 8c comparable to the reported complexes [43–45].

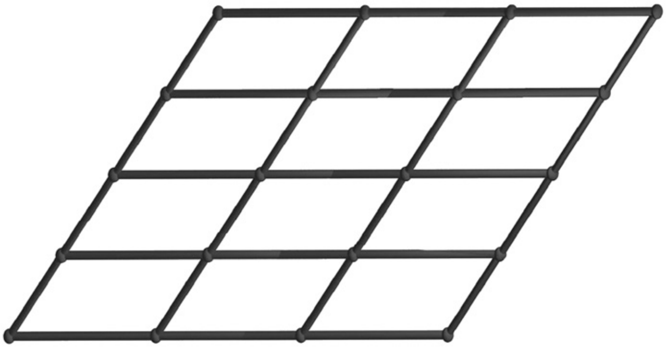

Fig. 6. Topological view of the 2D parallelogrammic grid of compound **2**.

Compared with compounds **1**–**3,** three (mono-, bi- and trinuclear) structural units are formed, respectively, which are further extended into 2D or 3D framework by bdc and **L** ligands. The effects of **L** and co-ligands on the ultimate structures and properties of these products are obvious. The **L** ligand prefers to coordinate with metal ions in the bridging mode compared with H_2biim and exhibits diverse conformational geometries when coordinates with different metal centers, which contribute to the formation of the three distinct compounds. Diverse coordination modes of bdc isomers effecting on the final structural arrays are also critical in the direction of the three novel frameworks. The bis-chelating coordination mode of *m*-bdc contributes to the formation of mononuclear structure units in compound **1,** while in compound **2**, the *m*-bdc ligand adopts the chelating–bridging coordination mode inducing the formation of binuclear subunits, and in compound **3**, the diverse coordination modes and the smaller angle between the two carboxylate groups of *p*-bdc result in the formation of trinuclear clusters, which contribute to the construction of compound **3**. In addition, the different metal ions radii and different reaction molar ratios also play important roles in the construction of the three novel structures.

3.2. XRPD patterns

The XRPD patterns for compounds **1** and **3** are presented in Figs. S1 and S2. The diffraction peaks of both simulated and experimental patterns match well in key positions, confirming the phase purities of compounds **1** and **3**.

3.3. Luminescent properties

Metal complexes are promising luminescent materials for their potential applications such as light-emitting materials (LEMs) owing to their abilities to enhance, shift and quench luminescent emissions of organic ligands by metal coordination [46]. The solid-state fluorescence spectra of **L** ligand, compounds **1** and **3** were observed at room temperature (shown in Fig. 9). The emission of **L** shows green fluorescence at 551 nm (upon

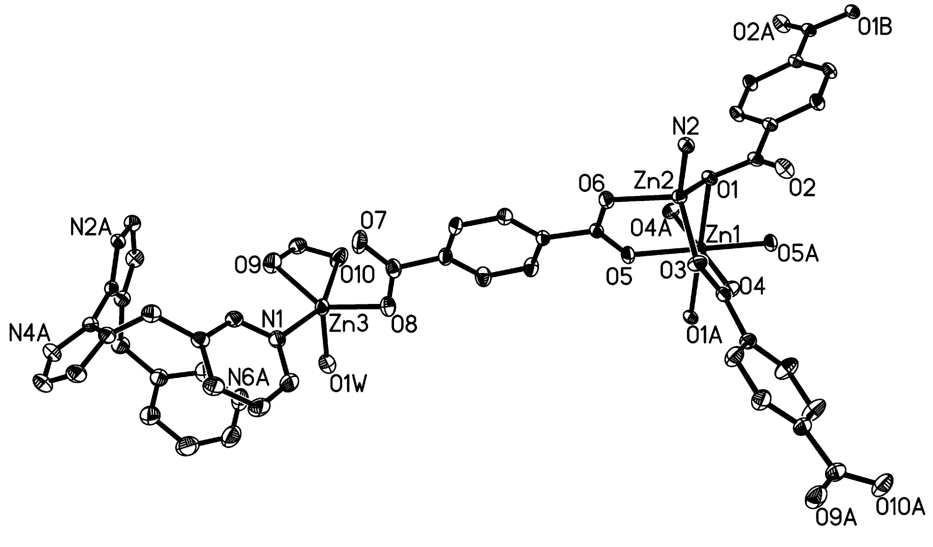

Fig. 7. ORTEP drawing of the coordination environment of zinc ion in compound **3** with thermal ellipsoids at the 30% probability level. H atoms are not shown for clarity.

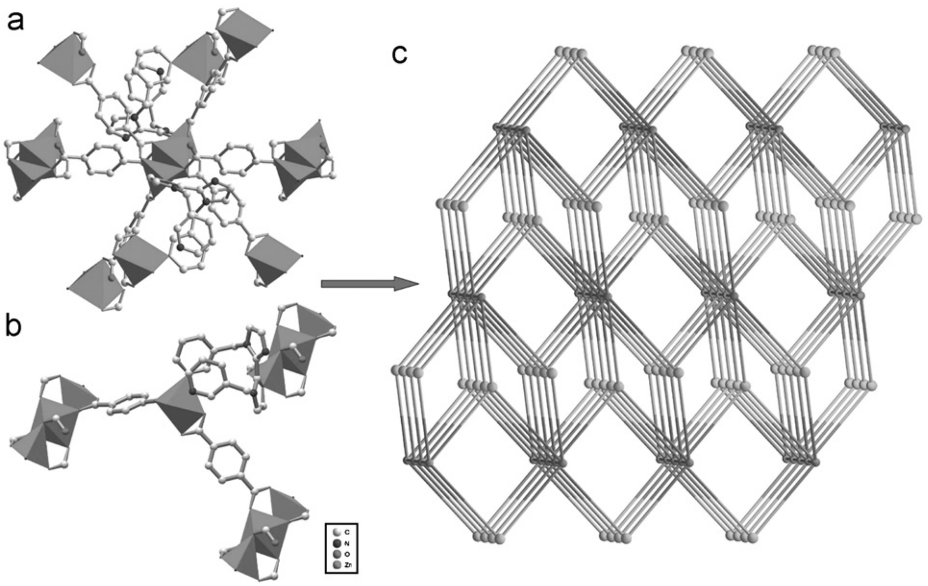

Fig. 8. (a) Polyhedral presentation of the trinuclear unit in compound **3** acting as a 8-connected node linked by *p*-bdc and **L** ligands. (b) Polyhedral presentation of five-coordinated metal center in compound **3** acting as a 3-connected node. (c) Topological view of the (3,8)-connected framework of structure **3**.

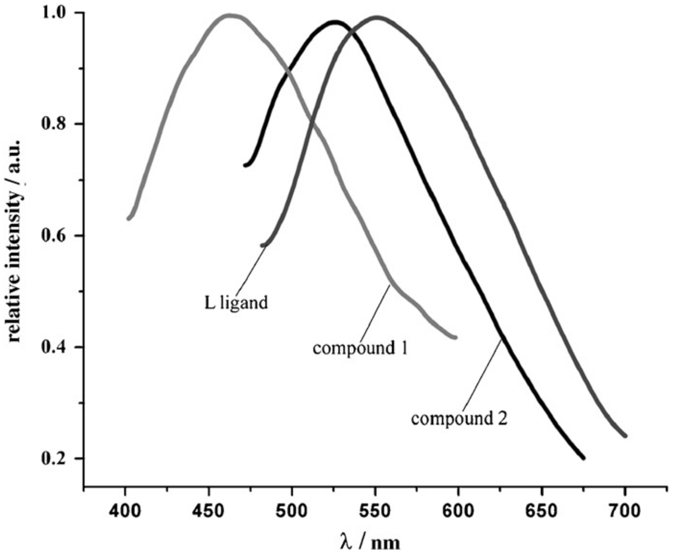

Fig. 9. Solid-state emission spectra of the **L** ligand, compounds **1** and **3** at room temperature.

excitation at 460 nm), which can be attributed to the $\pi^* \rightarrow \pi$ transition. Solid-state carboxylate ligands, *p*-bdc and *m*-bdc can also exhibit fluorescent properties at room temperature reported by the literature [47], and the emission bands of these carboxylate ligands can be assigned to the $\pi^* \rightarrow n$ transition. Compound **1** shows a single emission signal at 463 nm (upon excitation at 380 nm) exhibiting blue fluorescence and compound **3** exhibits green fluorescence at 526 nm (upon excitation at 450 nm). Compared with the emission of the free ligand, blue shift (88 nm for **1** and 25 nm for **3**) has been observed upon the formation of compounds **1** and **3** comparable to the reported literature [48]. It is well-known that the $\pi \rightarrow \pi^*$ transition is stronger than the $\pi^* \rightarrow n$ transition, and furthermore, the strong electron withdrawing group of the carboxyl group results in fluorescence quenching, so carboxylate ligands almost have no contribution to the fluorescent emissions of compounds **1** and **3**. According to the above description, the emissions of the two compounds may be assigned to $\pi^* \rightarrow \pi$ transitions of the **L** ligand and ligand to metal charge transfer (LMCT) [49].

4. Conclusions

In this work, three novel coordination complexes have been successfully prepared under hydrothermal conditions by reaction of the **L** ligand, bdc isomers and different metal ions in distinct molar ratios. Three different attractive topological types were obtained: 2D (3,5)-connected framework with $(4^2 \cdot 6)(4^2 \cdot 6^7 \cdot 8)$ topology based on mononuclear structural unit (**1**), 2D (4,4) grid based on binuclear structural unit (**2**) and 3D (3,8)-connected with $(4^3)(4^6 \cdot 6^{18} \cdot 8^4)$ topology based on trinuclear and mononuclear structural units (**3**), which provide new examples of structural diversity and illustrate again the aesthetic diversity of coordination chemistry. The different coordination geometries of **L** are crucial for the formation of the three distinct frameworks. In addition, the smaller angle between two carboxylate groups in *m*-bdc compared to that in *p*-bdc resulting in the crowding of the groups and the diverse coordination behavior of bdc ligands, that is, it behaves as linear (*p*-bdc) or angular (*m*-bdc) building block effecting on the final structural arrays, are also critical in the direction of the three novel frameworks. Moreover, **L** ligand, compounds **1** and **3** display fluorescent properties, indicating that they may have potential applications as optical materials. Further work on the properties of this ligand and its metal complexes is being carried out in our laboratory.

5. Supplementary materials

Experimental powder XPRD patterns have been given in Figs. S1 and S2. Crystallographic data for the structural analysis have been deposited with the Cambridge Crystallographic Data Center, CCDC reference number: 664539 for **1**, 664540 for **2** and 664538 for **3**. These data can be obtained free of charge at: www.ccdc.cam.ac.uk/conts/retriewing.html (or from the Cambridge Crystallographic Data Center, 12, Union Road, Cambridge CB2 1EZ, UK; fax: +44 1223/336 033; E-mail: deposit@ccdc.cam.ac.uk).

Acknowledgments

We are grateful to the National Natural Science Foundation of China for financial support (Nos. 20373009 and 20573016), and to the foundation for Excellent Youth of Jilin, China (Grant no. 20050107).

Appendix A. Supplementary materials

The online version of this article contains additional supplementary data. Please visit doi:10.1016/j.jssc.2008.05.039.

References

[1] L. Carlucci, G. Ciani, D.M. Proserpio, Coord. Chem. Rev. 246 (2003) 247–289.
[2] X.L. Wang, C. Qin, E.B. Wang, Y.G. Li, Z.M. Su, L. Xu, L. Carlucci, Angew. Chem. Int. Ed. 44 (2005) 5824–5827.
[3] Y.B. Dong, P. Wang, J.P. Ma, X.X. Zhao, H.Y. Wang, B. Tang, R.Q. Huang, J. Am. Chem. Soc. 129 (2007) 4872–4873.
[4] Z.M. Hao, X.M. Zhang, Cryst. Growth Des. 7 (2007) 64–68.
[5] S. Kitagawa, R. Kitaura, S. Noro, Angew. Chem. Int. Ed. 43 (2004) 2334–2375.
[6] B.L. Chen, F.R. Fronczek, B.H. Courtney, F. Zapata, Cryst. Growth Des. 6 (2006) 825–828.
[7] M. Albrecht, Chem. Rev. 101 (2001) 3457–3497.
[8] Y.B. Dong, Y.Y. Jiang, J. Li, J.P. Ma, F.L. Liu, B. Tang, R.Q. Huang, S.R. Batten, J. Am. Chem. Soc. 129 (2007) 4520–4521.
[9] L.R. Hanton, K. Lee, J. Chem. Soc. Dalton Trans. (2000) 1161–1166.
[10] D.P. Martin, R.M. Supkowski, R.L. LaDuca, Inorg. Chem. 46 (2007) 7917–7922.
[11] P.L. Caradoc-Davies, D.H. Gregory, L.R. Hanton, J.M. Turnbull, J. Chem. Soc. Dalton Trans. (2002) 1574–1580.
[12] M. Sathiyendiran, C.H. Chang, C.H. Chuang, T.T. Luo, Y.S. Wen, K.L. Lu, Dalton Trans. (2007) 1872–1874.
[13] P.L. Caradoc-Davies, L.R. Hanton, K. Lee, Chem. Commun. (2000) 783–784.
[14] R.L. Sang, L. Xu, Eur. J. Inorg. Chem. (2006) 1260–1267.
[15] R.L. Sang, L. Xu, Inorg. Chem. 44 (2005) 3731–3737.
[16] W.M. Barnett, R.G. Baughman, H.L. Collier, W.G. Vizuete, J. Chem. Cryst. 29 (1999) 765–768.
[17] X.F. Wang, Y. Lv, T.A. Okamura, H. Kawaguchi, G. Wu, W.Y. Sun, N. Ueyama, Cryst. Growth Des. 7 (2007) 1125–1133.
[18] Y.M. Fu, Y.H. Zhao, Y.Q. Lan, Y. Wang, Y.Q. Qiu, K.Z. Shao, Z.M. Su, Inorg. Chem. Commun. 10 (2007) 720–723.
[19] B.Q. Ma, K.L. Mulfort, J.T. Hupp, Inorg. Chem. 44 (2005) 4912–4914.
[20] B.L. Chen, S.Q. Ma, E.J. Hurtado, E.B. Lobkovsky, C.D. Liang, H.G. Zhu, S. Dai, Inorg. Chem. 46 (2007) 8705–8709.
[21] D.N. Dybtsev, H. Chun, K. Kim, Angew. Chem. Int. Ed. 43 (2004) 5033–5036.
[22] J. Yang, J.F. Ma, Y.Y. Liu, S.L. Li, G.L. Zheng, Eur. J. Inorg. Chem. (2005) 2174–2180.
[23] S.A. Bourne, J.J. Lu, A. Mondal, B. Moulton, M.J. Zaworotko, Angew. Chem. Int. Ed. 40 (2001) 2111–2113.
[24] M. Du, X.J. Jiang, X.J. Zhao, Inorg. Chem. 46 (2007) 3984–3995.
[25] B.B. Ding, Y.Q. Weng, Z.W. Mao, C.K. Lam, X.M. Chen, B.H. Ye, Inorg. Chem. 44 (2005) 8836–8845.
[26] S.J. In, J.M. Kang, Bull. Korean Chem. Soc. 26 (2005) 112–1124.
[27] G.M. Sheldrick, SHLEXL97, Program for Crystal Structure Refinement, University of Göttingen, Germany, 1997.
[28] X. Shi, G.S. Zhu, Q.R. Fang, G. Wu, G. Tian, R.W. Wang, D.L. Zhang, M. Xue, S.L. Qiu, Eur. J. Inorg. Chem. (2004) 185–191.
[29] K. Ramírez, J.A. Reyes, A. Briceño, R. Atencio, Cryst. Eng. Commun. 4 (2002) 208–212.
[30] K.K. Kamar, L.R. Falvello, P.E. Fanwick, J. Kim, S. Goswami, Dalton Trans. (2004) 1827–1831.
[31] R.J. Hill, D.L. Long, M.S. Turvey, A.J. Blake, N.R. Champness, P. Hubberstey, C. Wilson, M. Schröder, Chem. Commun. (2004) 1792–1793.
[32] D.L. Long, A.J. Blake, N.R. Champness, C. Wilson, M. Schröder, J. Am. Chem. Soc. 123 (2001) 340–3402.
[33] C.A. Williams, A.J. Blake, P. Hubberstey, M. Schröder, Chem. Commun. 11 (2005) 5435–5437.
[34] N.F. Zheng, J. Zhang, X.H. Bu, P.Y. Feng, Cryst. Growth Des. 7 (2007) 2567–2581.
[35] D.P. Cheng, M.A. Khan, R.P. Houser, J. Chem. Soc., J. Chem. Soc. Dalton Trans. 11 (2002) 4555–4560.
[36] D.P. Martin, M.A. Braverman, R.L. LaDuca, Cryst. Growth Des. 7 (2007) 2609–2619.
[37] C.A. Williams, A.J. Blake, P. Hubberstey, M. Schröder, Chem. Commun. (2005) 5435–5437.
[38] X.W. Wang, J.Z. Chen, J.H. Liu, Cryst. Growth Des. 7 (2007) 1227–1229.
[39] J. Tao, X. Yin, Z.B. Wei, R.B. Huang, L.S. Zheng, Eur. J. Inorg. Chem. (2004) 125–133.
[40] B.H. Ye, B.B. Ding, Y.Q. Weng, X.M. Chen, Cryst. Growth Des. 5 (2005) 801–806.
[41] L. Pan, H.M. Liu, X.G. Lei, X.Y. Huang, D.H. Olson, N.J. Turro, J. Li, Angew. Chem. Int. Ed. 42 (2003) 542–546.
[42] A.L. Grzesiak, F.J. Uribe, N.W. Ockwig, O.M. Yaghi, A.J. Matzger, Angew. Chem. Int. Ed. 45 (2006) 2553–2556.
[43] Q.R. Fang, G.S. Zhu, M. Xue, J.Y. Sun, F.X. Sun, S.L. Qiu, Inorg. Chem. 45 (2006) 3582–3587.
[44] S.Q. Ma, H.C. Zhou, J. Am. Chem. Soc. 128 (2006) 11734–11735.
[45] L.H. Xie, S.X. Liu, C.Y. Gao, R.G. Cao, J.F. Cao, C.Y. Sun, Z.M. Su, Inorg. Chem. 46 (2007) 7782–7788.
[46] Y.S. Song, B. Yan, Z.X. Chen, J. Solid State Chem. 179 (2006) 4037–4046.
[47] X. Shi, G.S. Zhu, X.H. Wang, G.H. Li, Q.F. Fang, X.J. Zhao, G. Wu, G. Tian, M. Xue, R.W. Wang, S.L. Qiu, Cryst. Growth Des. 5 (2005) 341–346.
[48] Y.P. Tian, Y.M. Zhu, H.P. Zhou, P. Wang, J.Y. Wu, X.T. Tao, M.H. Jiang, Eur. J. Inorg. Chem. (2007) 345–351.
[49] V.W.W. Yam, K.K.W. Lo, Chem. Soc. Rev. 28 (1999) 323–334.